Mitigation of the Impact of High Plug-in Electric Vehicle Penetration on Residential Distribution Grid Using Smart Charging Strategies

Authors:

Chong Cao, Luting Wang, Bo Chen

Date Submitted: 2019-02-27

Keywords: power distribution system, plug-in electric vehicle (PEV) charging, GridLAB-D, demand response (DR)

Abstract:

Vehicle electrification presents a great opportunity to reduce transportation greenhouse gas emissions. The greater use of plug-in electric vehicles (PEVs), however, puts stress on local distribution networks. This paper presents an optimal PEV charging control method integrated with utility demand response (DR) signals to mitigate the impact of PEV charging to several aspects of a grid, including load surge, distribution accumulative voltage deviation, and transformer aging. To build a realistic PEV charging load model, the results of National Household Travel Survey (NHTS) have been analyzed and a stochastic PEV charging model has been defined based on survey results. The residential distribution grid contains 120 houses and is modeled in GridLAB-D. Co-simulation is performed using Matlab and GridLAB-D to enable the optimal control algorithm in Matlab to control PEV charging loads in the residential grid modeled in GridLAB-D. Simulation results demonstrate the effectiveness of the proposed optimal charging control method in mitigating the negative impacts of PEV charging on the residential grid.

Record Type: Published Article

Submitted To: LAPSE (Living Archive for Process Systems Engineering)

Citation (overall record, always the latest version):	LAPSE:2019.0333
Citation (this specific file, latest version):	LAPSE:2019.0333-1
Citation (this specific file, this version):	LAPSE:2019.0333-1v1

DOI of Published Version: https://doi.org/10.3390/en9121024

License: Creative Commons Attribution 4.0 International (CC BY 4.0)

energies

MDPI

Article

Mitigation of the Impact of High Plug-in Electric Vehicle Penetration on Residential Distribution Grid Using Smart Charging Strategies

Chong Cao [1], Luting Wang [2] and Bo Chen [1,2,*]

[1] Department of Electrical and Computer Engineering, Michigan Technological University, Houghton, MI 49931, USA; chongcao@mtu.edu

[2] Department of Mechanical Engineering-Engineering Mechanics, Michigan Technological University, Houghton, MI 49931, USA; lutingw@mtu.edu

* Correspondence: bochen@mtu.edu; Tel.: +1-906-487-3537

Academic Editor: Paras Mandal

Received: 25 July 2016; Accepted: 25 November 2016; Published: 3 December 2016

Abstract: Vehicle electrification presents a great opportunity to reduce transportation greenhouse gas emissions. The greater use of plug-in electric vehicles (PEVs), however, puts stress on local distribution networks. This paper presents an optimal PEV charging control method integrated with utility demand response (DR) signals to mitigate the impact of PEV charging to several aspects of a grid, including load surge, distribution accumulative voltage deviation, and transformer aging. To build a realistic PEV charging load model, the results of National Household Travel Survey (NHTS) have been analyzed and a stochastic PEV charging model has been defined based on survey results. The residential distribution grid contains 120 houses and is modeled in GridLAB-D. Co-simulation is performed using Matlab and GridLAB-D to enable the optimal control algorithm in Matlab to control PEV charging loads in the residential grid modeled in GridLAB-D. Simulation results demonstrate the effectiveness of the proposed optimal charging control method in mitigating the negative impacts of PEV charging on the residential grid.

Keywords: demand response (DR); GridLAB-D; plug-in electric vehicle (PEV) charging; power distribution system

1. Introduction

Greenhouse gas (GHG) emissions have caused global warming over the past 50 years [1]. In 2009, the United States set a goal to reduce U.S. GHG emissions to 17% below 2005 levels by 2020 [2]. To achieve this goal, government agencies have set standards to regulate GHG emissions from several primary GHG emission sources, including electricity production, transportation, industry, commercial and residential buildings, agriculture, and land use and forestry. Among these primary GHG emission sources, transportation generated around 27% of total CO_2 equivalent emissions in 2013 [3]. In addition, transportation accounts for about two-thirds of U.S. petroleum consumption [1]. From these data, it is obvious that the current transportation system is one of the major contributors to GHG emissions and fuel consumption. The potential solution to reduce the transportation GHG emissions and fuel consumption is vehicle electrification. The rapid growth of plug-in electric vehicles (PEVs), including plug-in hybrid electric vehicles (PHEV) and battery electric vehicles (BEVs), however, brings great challenges to today's power system. The uncontrolled PEV charging could add heavy burden on the power grid during peak load time periods. In residential distribution networks, the peak household load occurs during the evening time. If PEV owners immediately charge their vehicles when they arrive home, the additional PEV charging load could put the grid at risk of damage from overloading.

To effectively integrate PEVs with power grids, a number of researchers have studied the impact of PEV charging on distribution networks and investigated charging management strategies to reduce this impact. Liu et al. [4] provided a literature review of PEV charge and discharge scenarios and their impacts on distribution systems, including phase imbalance, power quality, transformer degradation, and failure. Bosovic et al. [5] analyzed the impacts of PEV charging on a medium voltage distribution network in the northeastern part of Bosnia and Herzegovina. The effects of PEV charging on voltage profiles, energy losses, and the violations of network operational constraints are simulated. Since the statistical data on average daily trip distance are not available for the Bosnia and Herzegovina area, this work assumes that all the PEVs have almost empty batteries when the charging starts. The minimum step of PEV charging time is 1 h because the load profiles are on an hourly basis. The simulation results show that PEV charging, especially for slow charging at private charging stations, significantly impacts the load profile of the power system. With 20% of PEV penetration and unregulated charging, the voltage profile falls below the limit of −10% (p.u.). The increase of PEV penetration rate leads to an increase of energy losses. Based on the analysis results, the authors point out that the regulation of PEV charging process is necessary for higher percentages of PEV penetration. Calderaro et al. [6] assessed the impact of electric vehicles (EVs) on a campus distribution network based on vehicle usage data. The parking data, such as vehicles' arrival times and parking duration are used to characterize the parking area occupancy. The state of charges (*SOCs*) of incoming vehicles are calculated based on the vehicle travel distances and type of route (urban, extra urban, highway, and Mixed). This increases the accuracy of the incoming PEV *SOC* estimation. Four incoming vehicle patterns are identified based on the analysis of available data. These patterns enable better prediction of EV charging power demand for different days of a week and different time periods of a semester. Monte Carlo simulations are carried out to evaluate the grid impact in terms of increased power consumption and voltage deviation. The simulation results show the increase of peak power at the delivery node and the drop of node voltage due to EV charging. Qian et al. [7] and Rautiainen et al. [8] used a statistical method to model EV battery charging and load demand in a distribution system. Argade et al. [9] and Hilshey et al. [10] investigated EV charging and its impact on distribution transformer aging. Meyer et al. [11] analyzed the voltage deviation caused by public charging stations and propose combining distributed generators with EV charging stations to reduce grid stress. With the continuous increase of PEV market penetration rate, the utilities have recognized the importance of understanding the regulatory needs to support vehicle grid integration (VGI) [12].

This paper proposes an optimal PEV charging control method integrated with utility signals, such as demand response (DR) load control [13], to mitigate the impact of PEV charging loads to several aspects of a grid, including load surge, distribution accumulative voltage deviation, and transformer aging. Severe bus voltage deviation causes the increase of power losses along the transmission lines of a distribution grid [14]. To ensure proper operation of a power system, American National Standards Institute (ANSI) C84.1-2011 [15] specifies the standard operating voltage range of 60 Hz power systems. Meanwhile, since the most expensive component of an electrical distribution system is the power transformer, upgrading the distribution power transformers dramatically increases the power grid cost. Therefore, transformer-level load surge, distribution accumulative voltage deviation, and transformer aging are selected to assess the impact of PEV charging to a distribution grid. The PEV charging load model in this paper is built based on a real-world travel survey data set, National Household Travel Survey (NHTS). The travel data-based PEV charging load modeling has been employed in much research [7,8], although different survey data sources are used. The presented model considers the stochastic nature of PEV home arrival time (or PEV charging start time) and the PEV home arrival *SOC*. Due to the limitation of NHTS data, the estimation of PEV home arrival *SOC* assumes that the battery *SOC* is linearly related to the distance that a vehicle traveled and is not able to include other factors, such as type of routes considered in [6]. A concept of PEV penetration rate is introduced to represent the different levels of PEV charging power demand. The performance of the proposed optimal PEV charging control method is evaluated with metrics, which have been used in previous research, such as

load surge [6,7], accumulative voltage deviation [5,6,11], and transformer aging [9,10]. The residential distribution network used in this study contains 120 houses and is modeled in GridLAB-D (U.S. Department of Energy (DOE) at Pacific Northwest National Laboratory (PNNL), Richland, WA, USA) [16], a power distribution system simulation and analysis tool. The optimization algorithm is programed in Matlab (MathWorks, Natick, MA, USA), which generates PEV charging control signals. These two software packages run synchronously to perform co-simulation of PEV charging control. The rest of the paper is organized as follows. Section 2 presents the stochastic modeling of PEV charging power demand. Section 3 introduces the modeling of residential distribution grid and the baseline household load. Section 4 theoretically analyzes the impact of uncontrolled PEV charging on a local distribution system. Section 5 discusses the proposed optimal PEV charging control method. Section 6 discusses the simulation results, and Section 7 concludes the presented work.

2. Stochastic Modeling of Plug-in Electric Vehicle Fleet Charging

A report on electric vehicle charging [17] suggests that most PEV owners leave for work in the morning and return home in the evening. If PEV owners begin to charge vehicles immediately when they return to home, PEV charging is likely to have the greatest effect on the residential grid during the evening time. To study this impact, National Household Travel Survey (NHTS) [18] results have been analyzed to build a realistic PEV charging load model for a fleet of PEVs. The key variables that are valuable for the modeling of PEV fleet charging load in home to home trip data are fitted in Figure 1. It is found that the vehicle home arrival time T_{AH} follows a normal distribution $T_{AH} \sim N(\mu_{AH} = 17.09, \sigma_{AH} = 2.28)$ as shown in Equation (1), where μ_{AH} is the mean and σ_{AH} is the standard deviation of home arrival time. The home to home travel distance d_{HH} follows a log-normal distribution $d_{HH} \sim N(\ln d_{HH}; \mu_{HH} = 2.82, \sigma_{HH} = 1.06)$ as shown in Equation (2), where μ_{HH} and σ_{HH} are mean and standard deviation of the natural logarithm of home to home travel distance, respectively. The *t*-tests have been conducted on both arrival time and the natural logarithm of the home-to-home trip distance from NHTS data, and proved the distribution fits normality at the 5% significance level. The distributions of T_{AH} and d_{HH} are shown in Figure 1.

$$f_{T_{AH}}(T_{AH}) = \frac{1}{\sqrt{2\pi}\sigma_{AH}} e^{-\frac{(T_{AH}-\mu_{AH})^2}{2\sigma_{AH}^2}} \quad (1)$$

$$f_{d_{HH}}(d_{HH}) = \frac{1}{d_{HH}\sqrt{2\pi}\sigma_{HH}} e^{-\frac{(\ln(d_{HH})-\mu_{HH})^2}{2\sigma_{HH}^2}} \quad (2)$$

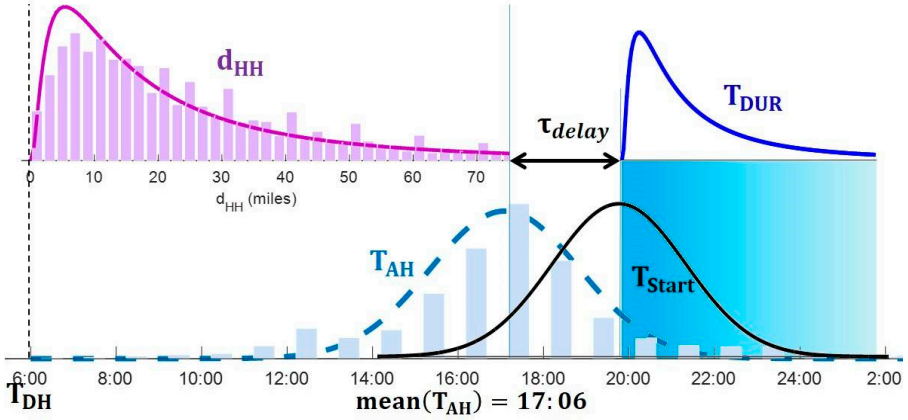

Figure 1. Stochastic modeling of plug-in electric vehicle (PEV) travel distance and charging schedule.

PEV charging start time T_{Start} and PEV charging duration T_{DUR} can be found from T_{AH} and d_{HH}. Assume that there is a time delay τ_{delay} between home arrival time T_{AH} and PEV charging start time T_{Start}. Charging start time can be represented as $T_{Start} = T_{AH} + \tau_{delay}$. It also follows a normal distribution $T_{Start} \sim N\left(\mu_{Start} = \mu_{AH} + \tau_{delay}, \sigma^2_{Start} = \sigma^2_{AH}\right)$. The PEV charging load duration is closely related to the PEV *SOC* at charging start time and the charging level of a charger. The PEV home arrival *SOC* depends on various factors, including the geographical factors of the trip, such as trip length, altitude variation, and traffic jams; the battery specification factors, such as battery type, battery aging, and charging/discharging efficiency; and the PEV specification factors and the environmental factors, such as the weather conditions and the ambient temperature [19]. Among these factors, the NHTS data set only provides the travel distance, which could be used to estimate the PEV home arrival *SOC*. Due to the limitation of the data source, it is assumed that the battery *SOC* is linearly related to the distance that a vehicle traveled and that the battery is fully charged before leaving home. The home arrival *SOC* of the charging batteries can be obtained by the statistics of vehicle home-to-home travel distance d_{HH} and the charging duration of the corresponding vehicle is shown in Equation (3).

$$T_{DUR} = \frac{E_{Demand}}{p_{level}} = \frac{E_{BS} d_{HH}}{p_{level} d_{EPA}} \tag{3}$$

where E_{BS}, p_{level}, and d_{EPA} are full battery size, charging rate, and Untied States Environmental Protection Agency (EPA) PEV driving range, respectively. In this study, the charging duration is estimated with a Nissan Leaf 2013 battery and an alternating current (AC) level 2 charger. From the Nissan site, the full battery size $E_{BS} = 24$ kWh, $d_{EPA} = 75$ miles and $p_{level} = 6.6$ kW. By fitting its samples, charging duration T_{DUR} follows a log-normal distribution $T_{DUR} \sim N(\ln T_{DUR}; \mu_{DUR}, \sigma_{DUR})$, where $\mu_{DUR} = 0.155$ and $\sigma_{DUR} = 1.06$ are the natural logarithms of mean and standard deviation of the charging duration random variable, respectively.

A joint random variable (T_{Start}, T_{DUR}) is formed to express the PEV fleet charging load. Since T_{Start} and T_{DUR} are independent, the probability density function (PDF) of the joint random variable (T_{Start}, T_{DUR}) can be defined by Equation (4), and the PDF plot is shown in Figure 2.

$$f(T_{Start}, T_{DUR}) = f_{T_{Start}}(T_{Start}) f_{T_{DUR}}(T_{DUR}) = \frac{1}{T_{DUR} 2\pi \sigma_{DUR} \sigma_{AH}} e^{-\frac{(T_{start} - (\mu_{AH} + \tau_{delay}))^2}{2\sigma^2_{AH}} - \frac{(\ln T_{DUR} - \mu_{DUR})^2}{2\sigma^2_{DUR}}} \tag{4}$$

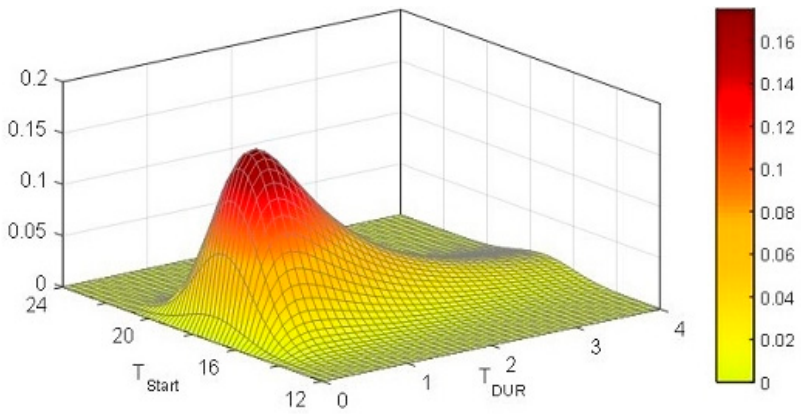

Figure 2. Joint distribution of charging start time and PEV charging duration.

With this joint random variable (T_{Start}, T_{DUR}), the PEV fleet charging load can be modeled by Equation (5):

$$p_{ev,i,j}(t, T_{Start}, T_{DUR}) = \begin{cases} \beta_{i,j} \cdot p_{level} & , \forall t \in [T_{Start}, T_{Start} + T_{DUR}] \\ 0 & , \forall t \notin [T_{Start}, T_{Start} + T_{DUR}] \end{cases} \tag{5}$$

where p_{level} is the charging rate for the selected charging level, as defined by the Society of Automotive Engineers (SAE) standard J1772 [20]. $\beta_{i,j}$ is a current factor that controls the actual PEV charging current through J1772 control pilot. In uncontrolled charging conditions, $\beta_{i,j} = 100\%$.

3. Residential Distribution Grid for Impact Study

The residential distribution grid used to study the impact of PEV charging is shown in Figure 3. The distribution grid is a modified Institute of Electrical and Electronics Engineers (IEEE) 13-node test feeder [21,22] connected to 120 houses. Node 650 together with a voltage regulator are modeled as the distribution substation in which a transformer converts 7200 V three-phase voltage down to 2400 V three-phase distribution voltage. Node 634 is a three-phase transformer, shifting voltage supply from phase to phase of 4160 V to 480 V. The rest of the nodes are connected to a single-phase residential load through residential split transformers. Three-phase four-line transmission lines between nodes are modeled by a π-equivalent line model. There are capacitor banks connected to nodes 611 and 675. Residential transformers are crucial components that transfer a substation level of 2400 V high voltage to 120 V residential voltage. Distribution transformers are center-tapped, with the primary connected with one of three phases from transmission and secondary outputs 120 V split-phase AC residential-level power. In Figure 3, there are 15 distribution transformers that are distributed to a total of 120 houses. A single-distribution transformer is 25 kVA load-rated and distributes electric power to a group of 8 houses.

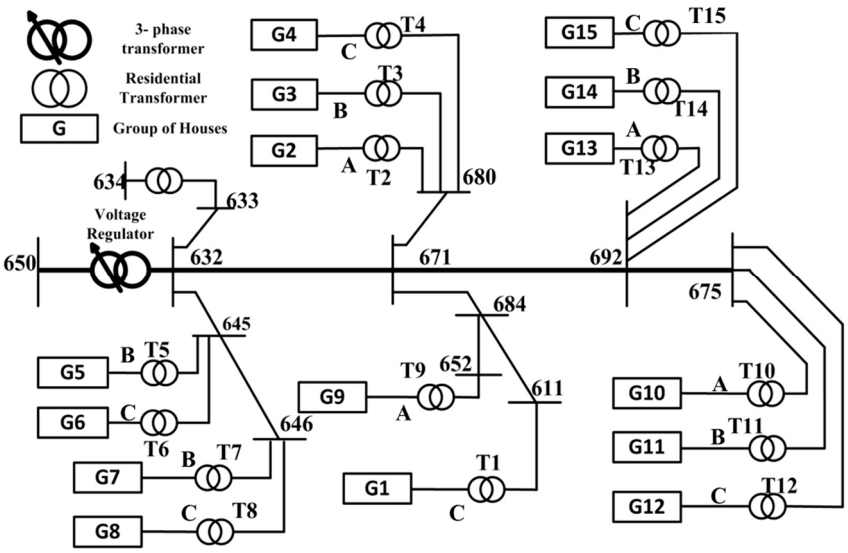

Figure 3. Residential distribution grid for impact study.

3.1. Residential Baseline Load Modeling

Household baseline load represents daily power usage of classical houses, including light load, heating, ventilating, and air conditioning load and other household appliance loads. In the distribution grid model, the baseline load profile is obtained from a "residential hourly load profile" of a specific typical meteorological year version 3 (TMY3) location in the United States, published by the National Renewable Energy Laboratory [23]. High temperature is an important factor that aggravates the aging of a distribution transformer. The high temperature also results in higher residential load especially consumed by heating, ventilation, and air conditioning systems (HVAC). Table 1 lists the monthly average residential house load [23] and average temperature variation in Arizona, Phoenix. July is the hottest month, therefore, the residential load profile in July is selected as the residential baseline load for the analysis in this paper.

Table 1. Monthly average residential load and ambient temperature in Arizona, Phoenix.

Month	Average Load (kW)	Temperature High (F)	Temperature Low (F)
January	0.97	67	46
February	0.95	71	49
March	0.86	77	53
April	1.05	85	60
May	1.39	95	69
June	1.99	104	78
July	2.25	106	83
August	2.17	104	83
September	2.01	100	77
October	1.33	89	65
November	0.88	76	53
December	0.96	65	45

3.2. Power Demand at Transformer

The load of an individual house can be modeled as the summation of PEV charging load and household baseline load. The Nissan Leaf 2013 with 24 kWh battery size and 6.6 kW charging rate has been modeled into residential houses according to different PEV penetration rates. We assume that PEVs with different penetrations will be uniformly distributed under all 15 transformers. Equation (6) shows the power demand at transformer i.

$$p_{T,i}(t) = \sum_{j=1}^{N_{H,i}} \left(\lambda_{i,j} \cdot p_{ev,i,j}(t, T_{Start,i,j}, T_{DUR,i,j}) + p_{base,i,j}(t) \right) \tag{6}$$

where $\lambda_{i,j}$ is a Boolean that specifies if the house j under transformer i has a PEV or not. The number of charging PEVs depends on PEV penetration rate. The $\lambda_{i,j} \cdot p_{ev,i,j}(t, T_{Start,i,j}, T_{DUR,i,j})$ expression is the PEV load of house j under transformer i. The charging time is specified by a joint random variable $(T_{Start,j}, T_{DUR,j})$. The $p_{base,i,j}(t)$ variable is the baseline load of the jth house. $N_{H,i}$ is the total number of houses under the transformer i.

4. Impact of Plug-in Electric Vehicle Charging on Residential Distribution Grid

4.1. Load Surge

The introduction of PEV brings additional loads to the distribution network and the increase of PEV penetration into the market in recent years aggravates this problem. The added PEV charging loads may cause the total residential loads to exceed the designed capacity of local distribution network transformers, which could lead to severe network performance deterioration and the damage of the electricity supply facility.

4.2. Voltage Deviation

Power flow analysis in power systems provides information about node voltage, power loss, and other factors in distribution networks. According to [14], voltage and current variation between nodes can be calculated by modeling transmission lines between two nodes, a π-equivalent circuit. Three-phase transmission lines between nodes have been modeled as a phase impedance matrix and a phase shunt admittance matrix. Voltage and current relation between two consecutive nodes $k-1$ and k can be represented as:

$$U_{k-1} = [a]U_k + [b]I_k \tag{7}$$

where $[a] = [u] + \frac{1}{2}[Z_{ABC}]_{k-1,k}[Y_{ABC}]_{k-1,k}$, $[b] = [Z_{ABC}]_{k-1,k}$, and $[u]$ is an identical matrix; $[Z_{ABC}]_{k-1,k}$ and $[Y_{ABC}]_{k-1,k}$ are the impedance matrix and shunt acceptance matrix of transmission line between

node $k-1$ and k, respectively. Since the second part of $[a]$, $\frac{1}{2}[Z_{ABC}]_{k-1,k}[Y_{ABC}]_{k-1,k}$, is much smaller than $[Z_{ABC}]_{k-1,k}$, voltage deviation between these two nodes can be expressed as a function of lower level node current as shown in Equation (8).

$$\Delta U_{k-1,k} = [Z_{ABC}]_{k-1,k} \sum_{j_k}^{N_k} I_{k,j_k} \tag{8}$$

where N_k is the total number of direct downstream branches of node k. By adding all voltage drops of adjacent nodes, the accumulative voltage deviation from the beginning node to any node k can be calculated by:

$$\Delta U_{1,k} = \sum_{k=2}^{K} \Delta U_{k-1,k} = \sum_{k=2}^{K} \sum_{j_k}^{N_k} [Z_{ABC}]_{k-1,k} I_{k,j_k} \tag{9}$$

In a power flow analysis, all the load will be converted to the equivalent current form. Therefore, Equation (9) indicates that heavy load will cause a deep voltage deviation in a circuit branch.

4.3. Impact on Local Transformer Aging

IEEE Standard C57.91-2011 [24] provides a mathematical modeling method to estimate the oil-immersed transformer insulation loss of life caused by the rise of electricity load and ambient temperature. Based on the standard, the deterioration of the mineral-oil-immersed transformer insulation is a time function of several factors, such as temperature, moisture, and oxygen. In these factors, the insulation temperature is a dominating factor, while the effect of moisture and oxygen can be minimized by modern techniques. Equation (10) shows the relation between the normalized transformer insulation life span and the hottest-spot winding temperature [24]:

$$Per\_Unit\_Life = 9.8 \times 10^{-18} e^{\frac{15000}{\theta_H + 273}} \tag{10}$$

where θ_H denotes the winding hottest-spot temperature. Per_Unit_Life denotes the normalized life span of transformer insulation at temperature θ_H. At reference temperature 110 °C, $Per\_Unit\_Life = 1$. The inverse of Per_Unit_Life is an important parameter, called aging acceleration factor.

$$F_{AA} = \frac{1}{Per\_Unit\_Life} = e^{\frac{15000}{383} - \frac{15000}{\theta_H + 273}} \tag{11}$$

Aging acceleration factor measures the impact of winding hottest-spot temperature on the transformer insulation life. The percentage loss of life can be calculated by:

$$Loss_{Life} = \frac{\sum_{n=1}^{N_T} F_{AA} \Delta t_n}{L_N} \tag{12}$$

where $Loss_{Life}$ is the percentage loss of life; L_N is the normal insulation life—usually, normal insulation life span of distribution transformer is designed to be 180,000 h or more.

According to IEEE Standard C57.91-2011 [24], winding hottest-spot temperature can be represented as:

$$\theta_{\mathrm{H}} = \theta_{AM} + \Delta\theta_{TO} + \Delta\theta_H \tag{13}$$

where θ_{AM} is the ambient temperature, $\Delta\theta_{TO}$ is the top-oil rise over ambient temperature, and $\Delta\theta_H$ is the winding hottest-spot rise over top-oil temperature. In Equations (14) and (15), $\Delta\theta_{TO}$ and $\Delta\theta_H$ are expressed as:

$$\Delta\theta_{TO} = (\Delta\theta_{TO,U} - \Delta\theta_{TO,I})(1 - e^{-\frac{t}{\tau_{TO}}}) + \Delta\theta_{TO,I} \tag{14}$$

$$\Delta\theta_H = (\Delta\theta_{H,U} - \Delta\theta_{H,I})(1 - e^{-\frac{t}{\tau_W}}) + \Delta\theta_{H,I} \tag{15}$$

In Equation (14), $\Delta\theta_{TO,I}$ and $\Delta\theta_{TO,U}$ are the initial and ultimate top-oil rise over ambient temperature and τ_{TO} is the top-oil time constant. τ_{TO} measures how fast the temperature varies between the initial and ultimate top-oil temperature and can be expressed as:

$$\tau_{TO} = \tau_{TO,R} \frac{\frac{\Delta\theta_{TO,U}}{\Delta\theta_{TO,R}} - \frac{\Delta\theta_{TO,I}}{\Delta\theta_{TO,R}}}{\left(\frac{\Delta\theta_{TO,U}}{\Delta\theta_{TO,R}}\right)^{\frac{1}{n}} - \left(\frac{\Delta\theta_{TO,I}}{\Delta\theta_{TO,R}}\right)^{\frac{1}{n}}} \tag{16}$$

where n is an empirically derived exponent specified by different cooling types. $\tau_{TO,R}$ is the time constant for rated load, beginning with initial top-oil temperature rise of 0 °C, and can be calculated by:

$$\tau_{TO,R} = \frac{C \times \Delta\theta_{TO,R}}{p_{T,R}} \tag{17}$$

where $p_{T,R}$ is the transformer total loss at rated load in watts. C is the thermal capacity of the transformer, which can be calculated by:

$$C = 0.06M_{CC} + 0.04M_{Tank} + 1.33V_{Oil} \tag{18}$$

where M_{CC} is the weight of the core and coil in pounds, M_{Tank} is the weight of the transformer tank in pounds, and V_{Oil} is the volume of oil in the transformer cooling system in gallons.

Similarly, in Equation (15), τ_W is the winding-time constant that measures speed of winding hottest-spot temperature change between initial winding hottest-spot temperature rise $\Delta\theta_{H,I}$ and ultimate winding hottest-spot temperature rise $\Delta\theta_{H,U}$. $\Delta\theta_{TO,U}$ and $\Delta\theta_{H,U}$ can be expressed by instant transformer load, as shown in the equations below:

$$\Delta\theta_{TO,U} = \Delta\theta_{TO,R}\left(\frac{K_U^2 R + 1}{R + 1}\right)^n \tag{19}$$

$$\Delta\theta_{H,U} = \Delta\theta_{H,R} K_U^{2m} \tag{20}$$

$$K_U = \frac{p_{T,i}(n\Delta t)}{25\,\text{kW}} \tag{21}$$

where $\Delta\theta_{TO,R}$ is the top-oil rise over ambient temperature at rated load. $\Delta\theta_{H,R}$ is the winding hottest-spot rise over top-oil temperature at transformer rated load on the tap position to be studied. R is the ratio of load loss at rated load to no load loss. K_U is the ratio of ultimate load to nominal transformer load. n and m are experimentally determined exponents specified by the transformer cooling mode.

Based on the discussion above, the impact of PEV charging on local distribution transformer insulation aging can be evaluated by the value of winding hottest-spot temperature θ_H. The value of θ_H is closely related to the instant transformer load. The whole process can be calculated by Equations (13)–(21) with parameters obtained from Turan Gönen's Electric Power Distribution System Engineering [25], GridLAB-D [26] recommended values, and IEEE Standard C57.91-2011 [24], as listed in Table A1 in Appendix A.

5. Managed Plug-in Electric Vehicle Charging with Smart Charging Strategies

The rapid growth of PEVs presents a new challenge to existing power grids due to the massive power drawn by PEV charging. To deal with this problem, utilities have developed various strategies. For example, DR programs offer time-based rates programs and the direct load control (DLC) program to engage customers in DR events. Considering a price-based time of use program (ToU) DR signal, shown in Figure 4, the utility charges higher prices during the afternoon and evening peak hours,

while charging lower prices during the morning and late night off-peak hours. Customers in this program know in advance the price schedule of their residential electricity usage, and tend to shift their PEV charging to off-peak hours, which reduces both the customer electricity bill and the impact from load aggregation. For the DLC-based PEV charging control, utilities can curtail or stop PEV charging by specifying allowable charging rates based on grid conditions.

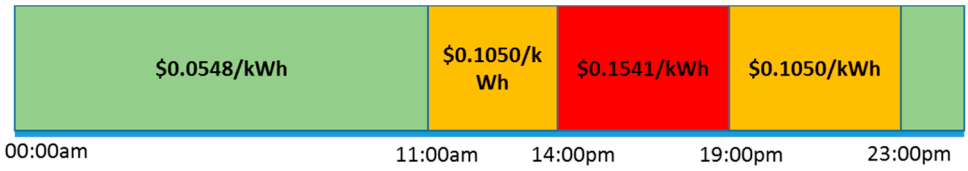

Figure 4. Time of use program (ToU) demand response (DR) signal for a summer day.

This paper presents an optimal PEV charging control method with constraints of ToU and DLC. The PEV charging management can be seen as a charging path searching problem. Assume that all PEVs begin the charging process at a "start time" according to the real-time pricing and DLC signal, and finish charging at a customer-specified "stop time". Individual PEVs have different initial *SOC* levels but the same target *SOC* values. Figure 5 shows an envelope of possible PEV charging paths confined by both ToU and DLC signals, in which the x-axis represents the time and the y-axis represents PEV battery *SOC*. The blue curve on the left is the earliest charging path between points A and B. With this path, a PEV is charged with largest allowable charging rate continuously until the target *SOC* is reached. Any path on the left side of the blue path is not allowed due to the DLC signals. The red path represents the latest possible charging path for a PEV to be charged from initial *SOC* to target *SOC* within a specified charging period. With the red path, the charging is not started until the last possible time to finish charging by following the DLC signals.

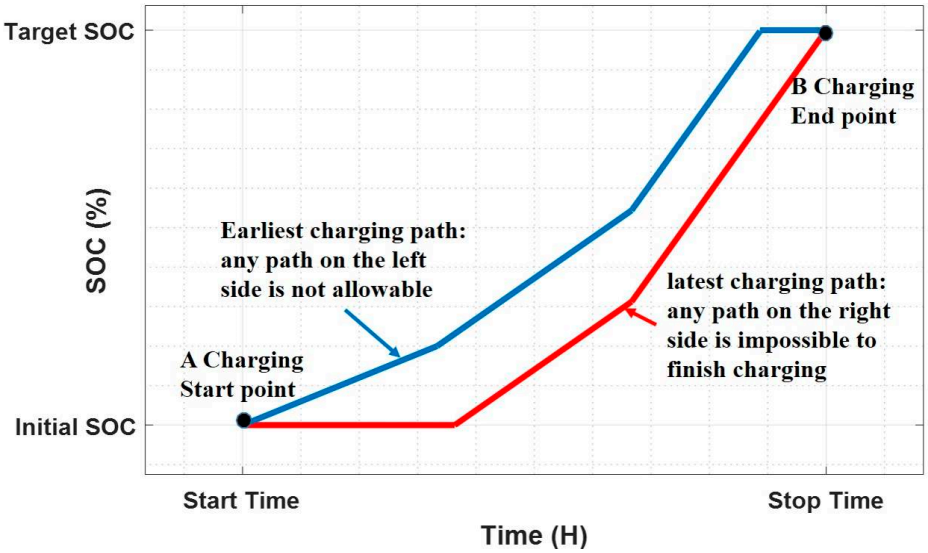

Figure 5. Envelope of PEV charging paths.

The slope of the PEV charging path in each time interval must be either zero (charger switch is off) or the PEV charging rate corresponding to DLC signals within different time periods. The goal of the proposed optimal charging control is to find a proper PEV charging path within this envelope, which reduces the transformer-level load surge and mitigates the impact of PEV charging to the distribution network. To achieve this goal, the objective function is defined to minimize the maximum transformer load during the charging time period, as shown in Equation (22). t_k is the time step that has a 10-min

time interval. Constraint in Equation (23) guarantees that PEVs are charged to customer-desired target *SOC* with a tolerance of δ. We define δ = 3% in this study. Constraint Equation (24) confines the PEV charging rate to either switched off or following the DLC signal. $\beta_{i,j}(t_k)$ in Equation (26) represents the charging rate specified by a DLC signal. In this study, the DLC signal is defined to charge PEVs at 30% of AC level II charging rate (1.92 kW during 23:00–01:00), 50% of AC level II charging rate (3.3 kW during 01:00–03:00), and 100% of AC level II charging rate (6.6 kW during 03:00–05:00). $\alpha_{i,j}(t_k)$ in Equation (25) is the output of the optimal algorithm, which represent PEVs in either a charging-on or a charging-off situation.

$$\min_{t_k \in T_{CH}} [\max(p_{T,i}(t_k))] \tag{22}$$

subject to:

$$(SOC_T - \delta) \cdot E_{BS} \leq E_{init,i,j} + \sum_{t_k \in T_{CH}} p_{ev,i,j}(t_k) \cdot \Delta t \leq SOC_T \cdot E_{BS} \tag{23}$$

$$p_{ev,i,j}(t_k) = \begin{cases} \alpha_{i,j}(t_k) \cdot \beta_{i,j}(t_k) \cdot p_{\text{level}}(t_k) & \text{t}_\text{k} \in T_{CH} \\ 0 & \text{t}_\text{k} \notin T_{CH} \end{cases} \tag{24}$$

$$\alpha_{i,j}(t_k) = \begin{cases} 1 & \text{charge on} \\ 0 & \text{charge off} \end{cases} \tag{25}$$

$$\beta_{i,j}(t_k) = \begin{cases} 30\% & t_k \in [23:00, 1:00) \\ 50\% & t_k \in [1:00, 3:00) \\ 100\% & t_k \in [3:00, 5:00) \end{cases} \tag{26}$$

This optimization problem is solved by using a genetic algorithm. Firstly, the 10-min time step charging status, $\alpha_{i,j}(t_k)$, for each PEV forms a 36-element Boolean vector for the 6-h charging period from 23:00 to 05:00. For all the participants of ToU + DLC + optimal control program under the *i*th transformer, the combination of their charging status Boolean vectors forms a chromosome with a length of $36 \times J_i$, where J_i is the number of the participants under *i*th transformer. The genetic algorithm initiates the search of an optimal charging schedule by randomly generating a number of possible solutions as the first generation. The fitness of these solutions is evaluated by the fitness function defined in Equation (22). By ranking the individual solutions' fitness scaling, a number of solutions who best fit the fitness function (Equation (22)) and the constraints (Equations (23)–(26)) are selected to produce a new generation of solutions with the same population size through crossover and mutation schemes. The iteration is repeated until the stopping criterion is met. In this application, the genetic algorithm terminates execution when the value of fitness function has no improvement in 50 consecutive generations. With the same stopping criterion, repeated tests are conducted with various population sizes (500, 1000, 5000, 10000) to evaluate the effect of the population size on the computational time. For each population size, the test is repeated multiple times and the average of the computational time is pursued. The tests are conducted on an Intel(R) core i7-6700HQ CPU computer. The test results show that the smaller population size has the faster convergence speed. The average time of the test with 500 and 1000 population size are 16.76 and 50.18 seconds. However, when we rise the population size to 5000 and 10000, the tests take 116.61 seconds and 213.45 seconds to converge respectively. By considering the quality of the optimal solution and the computational time, the population size of 1000 is selected in this application.

By solving this minimization problem, a transformer-level controller finds the optimized charging scheduling for all the PEVs under this transformer in 10-min intervals.

6. Simulation Results

The co-simulation is performed using GridLAB-D and Matlab. GridLAB-D models the modified residential grid introduced in Section 3 and the power flow of the grid. The DR signals are simulated

in Matlab. Two software packages exchange data at each synchronization time instance. For the simplicity of analysis, we focus on phase C branch only, which has the heaviest load in this residential grid. We assume a high PEV penetration rate (i.e., 75%), that PEVs are evenly distributed in the grid, and all the PEV owners participate in the ToU and DLC programs. It is also assumed that only PEV charging load is controllable in this residential grid. In addition, we assume that all customers choose 05:00 as charging finish time and 100% *SOC* as target *SOC*. In this section, we present and analyze PEV charging process using four different charging scenarios and their impact on the performance of the distribution network and device aging.

A comparison study is conducted on PEV charging paths, load surge, voltage deviation, and transformer insulation aging of four PEV charging scenarios: the uncontrolled PEV charging, the ToU + DLC charging, the ToU + DLC + optimal charging, and the partial participation of controlled charging. For uncontrolled PEV charging, PEV owners charge their vehicles with an AC level II charging rate once they arrive home. The stochastic PEV fleet charging model established in Section 2 is used with the delay time $\tau_{delay} = 0$. For ToU + DLC method, the PEV charging starts at 23:00, and the charging rate follows DLC sigma $\beta_{i,j}(t_k)$ described in Section 5. The ToU + DLC + optimal charging scenario uses the genetic algorithm to find an optimal charging schedule with ToU and DLC constraints. For partial participation of a controlled charging scenario, 80% participation rate of the ToU + DLC + optimal charging is assumed (20% of uncontrolled charging). For the reasons discussed in Section 3.1, the hourly average residential house load profile in July is used as the baseline load of each residential house. The hourly average residential house load profile is calculated by averaging the load values for the same hour of each day in a month.

6.1. Charging Path

Figure 6a,b shows the PEV charging paths using uncontrolled PEV charging and ToU + DLC charging control methods, respectively.

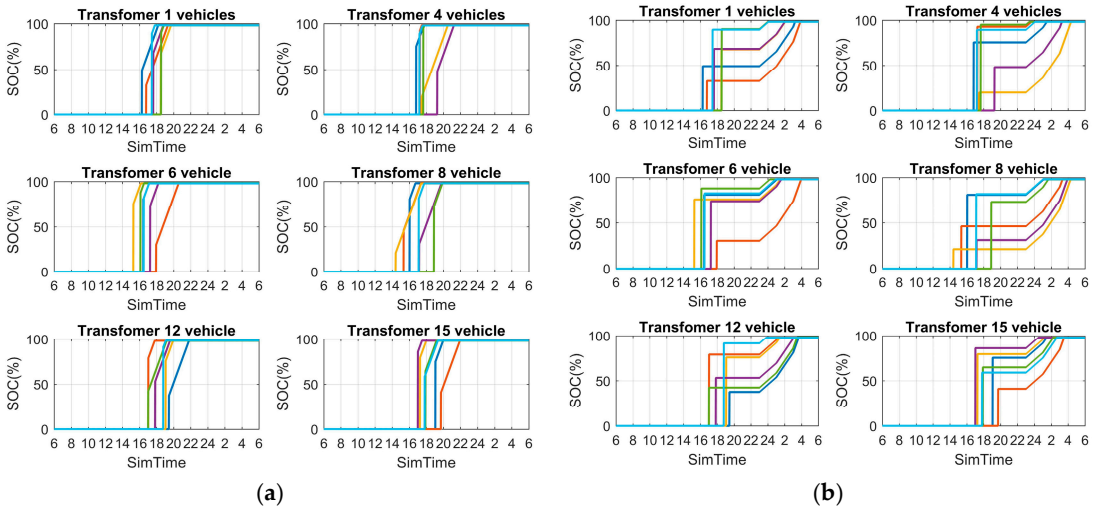

Figure 6. PEV charging paths under distribution transformers on phase C. (**a**) Uncontrolled PEV charging paths; and (**b**) PEV charging paths with ToU + direct load control (DLC) method.

Figure 7 shows the PEV charging paths using ToU + DLC + optimal charging and 80% of participation rate scenario (20% uncontrolled PEV charging). With ToU + DLC and ToU + DLC + optimal control methods, the charging processes of all PEVs are delayed until 23:00 to avoid both the aggregation of residential baseline load with PEV charging load and high charging price rate. Further comparing these two methods, the charging durations of some PEVs are extended in ToU + DLC + optimal control method to minimize the maximum power at individual transformers. However, all

the PEVs are charged to the target *SOC* before the end of charging duration in ToU + DLC + optimal control. In Figure 7b, 80% of the PEV owners choose the ToU + DLC + optimal control charging, while the remaining 20% utilize uncontrolled charging.

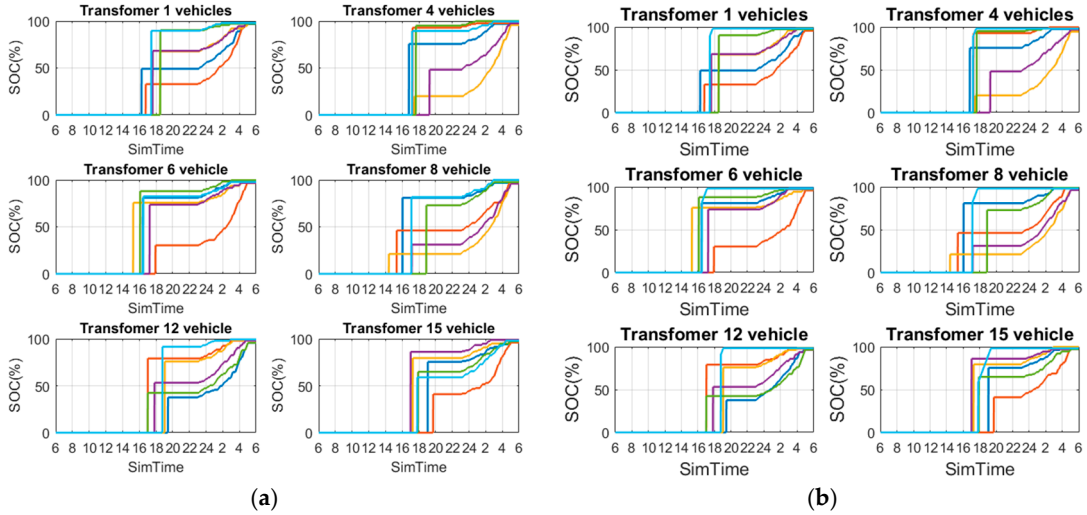

Figure 7. PEV charging paths with ToU + DLC + optimal charging. (**a**) A 100% participation rate optimal PEV charging scenario; and (**b**) an 80% participation rate of optimal PEV charging scenario (20% uncontrolled PEV charging).

6.2. Load Surge

Figure 8 shows the comparison of aggregated transformer-level load for the four charging scenarios. It is seen that, in an uncontrolled scenario, the aggregated loads in phase C transformers exceed 40 kW and mostly concentrate during 17:00–21:00. This heavy load is far beyond the nominal load of selected transformers, which is 25 kW. Both ToU + DLC charging and ToU + DLC + optimal control charging methods greatly mitigate the load surge by shifting the PEV charging load to off-peak hours and when the electricity price is the lowest in a day. However, without optimal control, the ToU + DLC charging still generates a few sudden load surges, especially at 23:00, 1:00, and 3:00. That is because at these time instances, the allowable charging rate rises dramatically and vehicles remain at their charging status until they are charged to a target *SOC*. The proposed ToU + DLC + optimal control method is designed to reduce the maximal value of the aggregated load and, as a result, eliminates the sudden load surge at charging rate transition time instances. For the 80% participation rate of ToU + DLC + optimal charging scenario, most PEV charging loads are shifted to the off-peak period. However, the 20% of uncontrolled PEV charging loads are aggregated with residential loads and results in 25–30 kW load surges during peak hours of the day. It is shown that the increase of participation rate of the ToU + DLC + optimal control method results in better load surge mitigation performance.

6.3. Voltage Deviation

According to the analysis in Section 4.2, voltage deviation decisively depends on the accumulative load of the branch. Figure 9 shows the secondary side metered voltage (also called service voltage) of distribution transformers in phase C. According to ANSI C84.1 [15], for 120 V service voltage Range A, voltage fluctuation should be confined within 114–126 V. From Figure 9, the uncontrolled charging has significant voltage deviation during the peak hours. During 17:00–20:00, the service voltage of transformers 1, 4, 12, and 15 drop below the lower threshold of 114 V. In ToU + DLC charging and ToU + DLC + optimal control charging, voltage deviation is largely reduced, especially with the ToU + DLC + optimal control charging strategy. This is because the ToU + DLC + optimal charging control minimizes the maximum power for individual transformers when making charging schedule

decisions. Similar to the situation in load surge analysis, the 80% participation rate of the optimal charging strategy slightly reduces the effectiveness of voltage deviation reduction.

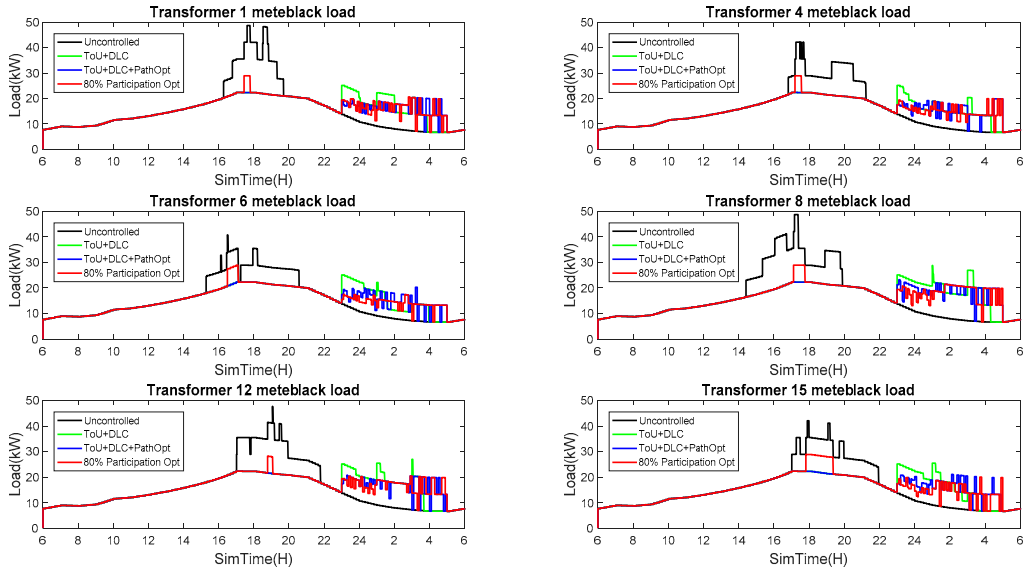

Figure 8. Transformer-level load profile for transformers in phase C with uncontrolled PEV charging, ToU + DLC charging, ToU + DLC + optimal control charging, and 80% participation rate of ToU + DLC + optimal control charging.

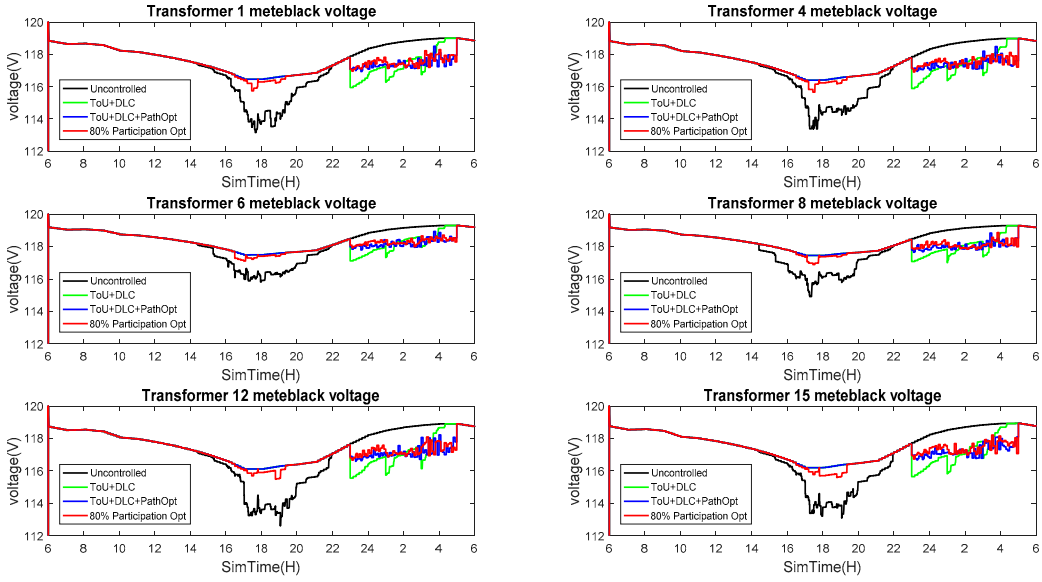

Figure 9. Service voltage deviation in uncontrolled charging, ToU + DLC charging, ToU + DLC + optimal control charging, and 80% participation rate of ToU + DLC + optimal control charging.

6.4. Transformer Insulation Aging

The loss of life of transformer insulation is one of key indicators of transformer aging. The nominal loss of life rate of a distribution transformer designed with a 20-year life span should be much less than 0.013% per day. Table 2 illustrates the one-day transformer internal insulation loss of life data in uncontrolled charging, ToU + DLC charging, ToU + DLC + optimal control charging, and 80% participation rate of optimal control charging. Because of aggregated load surge, the uncontrolled charging causes dramatic damage to the transformers, which leads to a severe transformer aging.

The ToU + DLC + optimal control charging method has the smallest transformer insulation loss of life due to the shifting of the PEV charging load and minimizing the total residential load, which allows the transformers to work in a healthy manner. When the participation rate of ToU + DLC + optimal control charging is 80%, though the load surge is partly mitigated, the remaining 20% of uncontrolled PEV charging loads and the baseline load cause transformers to be overloaded around 18:00, and this may shorten the transformer life spans. However, the amount of load surge is much smaller and the duration is much shorter compared with uncontrolled PEV charging, as shown in Figure 8, and thus, the impact on transformer aging is reduced compared with uncontrolled PEV charging.

Table 2. Distribution transformer internal insulation loss of life in one day (%).

Loss of Life in One Day	T1 [1] (10^{-3})	T4 (10^{-3})	T6 (10^{-3})	T8 (10^{-3})	T12 (10^{-3})	T15 (10^{-3})
Uncontrolled charging	700	66	32	377	207	89
ToU + DLC charging	1.80	1.70	1.80	2.10	1.90	1.90
ToU + DLC + optimal control charging	1.60	1.60	1.60	1.80	1.60	1.60
80% participation rate of optimal control charging (20% uncontrolled charging)	2.10	2.00	2.30	2.80	1.90	5.00

[1] T represents distribution transformer.

6.5. Seasonal Effect

The impact of PEV charging and the performance of optimal PEV charging control in all 12 months are investigated. Tables A2–A5 in Appendix A show the monthly simulation results of load surge, minimum voltage, and transformer insulation loss of life values for the four charging scenarios. It is clearly seen in the tables that, though uncontrolled PEV charging results in transformer-level overloading throughout the year, it causes more problems during summer months (May–September). In summer, the aggregated load surge could exceed 45 kW on a 25 kW rated distribution transformer for uncontrolled PEV charging. The line voltage is dramatically deviated from the 120 V nominal value, and exceeds the standard service voltage range of 114–126 V defined in ANSI C84.1 [15]. The transformer insulation aging simulation also shows that the transformer life loss in summer is greater than that in winter due to overloading and high ambient temperature. Tables A2–A5 in Appendix A also show that the ToU + DLC charging, ToU + DLC + optimal charging, and 80% participation rate of optimal charging can reduce/mitigate the impact of PEV charging with the ToU + DLC + optimal charging having the best performance.

7. Conclusions

This paper provides theoretical analysis of the impact of high penetration of uncontrolled PEV charging on electric distribution systems. An optimal charging control method is proposed with the consideration of utility DR (ToU and DLC) signals to mitigate the impact of aggregated residential and PEV charging load to several aspects of a grid, including load surge, voltage deviation and the aging of distribution transformers. From the simulation results, the proposed ToU + DLC + optimal charging control method effectively mitigates negative impacts by shifting the PEV charging load and minimizing the total residential load at individual transformer level. With this optimal PEV charging control, the distribution grid performs better compared to the uncontrolled charging and ToU + DLC charging.

Author Contributions: Each of the authors contributed to the research article. Chong Cao performed the simulation, analyzed the data, and wrote the paper. Luting Wang provided critical comments. Bo Chen supervised the related research work and finalized the manuscript.

Conflicts of Interest: The authors declare no conflict of interest.

Appendix A

Table A1. Transformer thermal and aging parameters used in the model.

Transformer Parameters	Value
Winding hottest-spot temperature over top-oil temperature at rated load, $\Delta\theta_{H,R}$	50 °C
Top oil temperature rise over ambient temperature at rated load, $\Delta\theta_{TO,R}$	30 °C
Ratio of load loss at rated load to no-load loss, R	2
Rated load loss $p_{T,R}$	0.006 (p.u)
Weight of the tank M_{tank}	60 (lb)
Weight of core and coil M_{cc}	50 (lb)
Volume of oil V_{Oil}	8.7 (gallon)
Winding time constant, τ_W	0.5 (h)
$\Delta\theta_{TO}$ exponent, n	0.8 ONAN
$\Delta\theta_H$ exponent, m	0.8 ONAN

Table A2. Summary of the impact of uncontrolled PEV charging in 12 months.

Grid Impact	Transformer	January	February	March	April	May	June	July	August	September	October	November	December
Load Surge	1	36.5798	35.62	34.33	37.82	42.11	47.94	48.69	48.63	47.39	40.43	36.09	36.86
	4	28.0463	27.23	26.23	31.18	35.51	41.38	42.11	42.03	40.8	33.68	27.79	28.47
	6	25.6855	25.27	24.67	29.73	34.16	40.04	40.77	40.64	39.45	32.59	25.43	25.87
	8	33.8089	33.12	32.27	37.62	42.1	47.98	48.71	48.62	47.4	40.28	33.58	34.18
	12	37.1278	36.16	34.79	37.79	41.45	47.04	47.74	47.65	46.42	40.6	36.53	37.3
	15	30.5278	29.56	28.31	31.26	35.52	41.31	42.09	42.04	40.78	34	29.93	30.7
Minimum line voltage	1	115.6	115.8	115.2	115.8	114.4	113.3	113.2	113.2	113.4	114.7	115.7	115.6
	4	115.9	116.1	115.4	116.1	114.6	113.5	113.4	113.4	113.6	114.9	116	115.9
	6	117.5	117.6	117.2	117.6	116.7	115.9	115.8	115.8	116	116.9	117.5	117.4
	8	116.9	117	116.4	117	115.8	115	114.9	114.9	115.1	116	116.9	116.8
	12	114.7	114.9	114.6	114.9	113.9	112.7	112.6	112.6	112.9	114	114.8	114.7
	15	115.2	115.3	115	115.3	114.3	113.2	113.1	113.1	113.4	114.5	115.3	115.1
Transformer aging—insulation loss of life (%)	1	2.39×10^{-4}	1.02×10^{-4}	3.95×10^{-4}	2.56×10^{-3}	1.48×10^{-2}	2.60×10^{-1}	6.97×10^{-1}	4.49×10^{-1}	2.23×10^{-1}	5.10×10^{-3}	4.54×10^{-4}	1.96×10^{-4}
	4	2.35×10^{-5}	1.09×10^{-5}	4.36×10^{-5}	2.36×10^{-4}	1.10×10^{-3}	2.05×10^{-2}	6.56×10^{-2}	3.97×10^{-2}	1.85×10^{-2}	3.79×10^{-4}	3.87×10^{-5}	1.66×10^{-5}
	6	6.58×10^{-6}	2.84×10^{-6}	1.76×10^{-5}	1.01×10^{-4}	5.03×10^{-4}	9.87×10^{-3}	3.24×10^{-2}	1.90×10^{-2}	9.00×10^{-3}	1.62×10^{-4}	1.56×10^{-5}	4.59×10^{-6}
	8	6.40×10^{-5}	2.97×10^{-5}	1.69×10^{-4}	1.34×10^{-3}	7.70×10^{-3}	1.34×10^{-1}	3.77×10^{-1}	2.40×10^{-1}	1.22×10^{-1}	2.50×10^{-3}	1.66×10^{-4}	4.37×10^{-5}
	12	9.53×10^{-5}	3.97×10^{-5}	1.37×10^{-4}	7.21×10^{-4}	3.90×10^{-3}	6.93×10^{-2}	2.07×10^{-1}	1.31×10^{-1}	6.24×10^{-2}	1.40×10^{-3}	4.69×10^{-5}	7.43×10^{-5}
	15	3.22×10^{-5}	1.33×10^{-5}	5.43×10^{-5}	2.86×10^{-4}	1.50×10^{-3}	2.84×10^{-2}	8.87×10^{-2}	5.42×10^{-2}	2.53×10^{-2}	5.10×10^{-4}	5.45×10^{-5}	2.47×10^{-5}

Table A3. Summary of the impact of ToU + DLC PEV charging in 12 months.

Grid Impact	Transformer	January	February	March	April	May	June	July	August	September	October	November	December
Load Surge	1	18.67	18.71	18.39	17.81	19.99	23.31	25.14	24.34	22.29	18.94	18.16	18.52
	4	18.67	18.71	18.39	17.81	19.99	23.31	25.14	23.34	22.29	18.94	18.16	18.52
	6	18.67	18.71	18.39	17.81	19.99	23.31	25.14	23.34	22.29	18.94	18.16	18.52
	8	23.68	23.74	23.35	23.05	24.3	26.62	28.79	28.07	27.09	23.99	23.3	23.62
	12	22.84	22.91	22.75	22.5	22.98	24.85	26.95	26.45	25.58	23.04	22.41	22.79
	15	20.28	20.44	20.25	19.75	21	23.31	25.49	24.77	23.79	20.69	20	20.32
Minimum line voltage	1	117.1	117	117.1	117.2	116.8	116.3	116	116.1	116.3	117	117.1	117.1
	4	117	117	117	117.1	116.8	116.2	115.9	116	116.3	117	117.1	117
	6	117.9	117.9	117.9	118	117.7	117.3	117.1	117.2	117.4	117.9	118	117.9
	8	117.6	117.6	117.7	117.7	117.6	117.3	117	117.1	117.2	117.6	117.7	117.6
	12	116.7	116.7	116.7	116.8	116.5	115.9	115.6	115.7	116.1	116.7	116.8	116.7
	15	116.9	116.7	116.8	116.9	116.6	116	115.7	115.8	116.1	116.6	116.8	116.8
Transformer Aging—insulation loss of life (%)	1	2.51×10^{-6}	1.06×10^{-6}	3.81×10^{-6}	1.25×10^{-5}	2.66×10^{-5}	4.08×10^{-4}	1.80×10^{-3}	9.30×10^{-4}	4.28×10^{-4}	1.33×10^{-5}	3.45×10^{-6}	2.07×10^{-6}
	4	1.54×10^{-6}	6.40×10^{-7}	3.81×10^{-6}	1.02×10^{-5}	2.44×10^{-5}	3.88×10^{-4}	1.70×10^{-3}	8.55×10^{-4}	3.94×10^{-4}	1.08×10^{-5}	3.45×10^{-6}	1.22×10^{-6}
	6	2.18×10^{-6}	9.22×10^{-7}	4.70×10^{-6}	1.17×10^{-5}	2.62×10^{-5}	4.07×10^{-4}	1.80×10^{-3}	9.20×10^{-4}	4.23×10^{-4}	1.25×10^{-5}	3.20×10^{-6}	1.74×10^{-6}
	8	4.63×10^{-6}	1.98×10^{-6}	8.33×10^{-6}	1.72×10^{-5}	3.04×10^{-5}	4.33×10^{-4}	2.10×10^{-3}	1.00×10^{-3}	4.79×10^{-4}	1.80×10^{-5}	3.85×10^{-6}	4.15×10^{-6}
	12	2.98×10^{-6}	1.26×10^{-6}	5.97×10^{-6}	1.35×10^{-5}	2.74×10^{-5}	4.13×10^{-4}	1.90×10^{-3}	9.56×10^{-4}	4.40×10^{-4}	1.44×10^{-5}	3.85×10^{-6}	2.53×10^{-6}
	15	2.93×10^{-6}	1.24×10^{-6}	5.86×10^{-6}	1.33×10^{-5}	2.76×10^{-5}	4.18×10^{-4}	1.90×10^{-3}	9.68×10^{-4}	4.45×10^{-4}	1.44×10^{-5}	3.82 × 10-6	2.42E-06

Table A4. Summary of the impact of ToU + DLC+ optimal PEV charging in 12 Months.

Grid Impact	Transformer	January	February	March	April	May	June	July	August	September	October	November	December
Load Surge	1	16.77	16.64	16.13	16.13	17.01	21.59	22.32	22.24	21	16.42	15.74	16.19
	4	16.22	16.29	16.13	15.9	16.29	21.59	22.32	22.24	21	16.42	15.78	16.18
	6	16.21	16.3	16.12	15.89	16.12	21.59	22.32	22.24	21	16.42	15.74	16.18
	8	16.46	19.68	16.12	16.13	22.57	24.42	22.32	22.24	21	19.96	19.25	20.32
	12	16.27	16.3	16.12	16.03	16.2	21.59	22.32	22.24	21	16.5	16.4	16.27
	15	16.23	16.29	16.26	16.13	16.3	21.59	22.32	22.24	21	16.5	15.74	16.27
Minimum line voltage	1	117.5	117.6	117.5	117.7	117.5	116.6	116.5	116.5	116.7	117.7	117.8	117.7
	4	117.5	117.6	117.5	117.7	117.5	116.5	116.4	116.4	116.6	117.7	117.9	117.7
	6	118.3	118.3	118.4	118.3	118.3	117.6	117.5	117.5	117.6	118.3	118.5	118.4
	8	118.2	118.2	118.3	118	118	117.6	117.5	117.5	117.6	118	118.4	118.2
	12	117.2	117.3	117.3	117.5	117.3	116.3	116.1	116.1	116.4	117.4	117.6	117.5
	15	117.3	117.4	117.4	117.6	117.3	116.3	116.2	116.2	116.4	117.5	117.7	117.6
Transformer Aging—insulation loss of life (%)	1	1.42×10^{-6}	5.93×10^{-7}	3.81×10^{-6}	9.78×10^{-6}	2.37×10^{-5}	3.76×10^{-4}	1.60×10^{-3}	8.26×10^{-4}	3.81×10^{-4}	1.04×10^{-5}	2.51×10^{-6}	1.25×10^{-6}
	4	1.21×10^{-6}	4.93×10^{-7}	3.81×10^{-6}	9.36×10^{-6}	2.32×10^{-5}	3.73×10^{-4}	1.60×10^{-3}	8.08×10^{-4}	3.73×10^{-4}	9.78×10^{-6}	2.31×10^{-6}	9.90×10^{-7}
	6	1.15×10^{-6}	4.90×10^{-7}	4.70×10^{-6}	9.14×10^{-6}	2.32×10^{-5}	3.73×10^{-4}	1.60×10^{-3}	8.06×10^{-4}	3.75×10^{-4}	9.91×10^{-6}	2.31×10^{-6}	9.26×10^{-7}
	8	2.72×10^{-6}	1.14×10^{-6}	8.33×10^{-6}	1.37×10^{-5}	2.59×10^{-5}	3.91×10^{-4}	1.80×10^{-3}	8.91×10^{-4}	4.05×10^{-4}	1.33×10^{-5}	3.59×10^{-6}	2.65×10^{-6}
	12	1.65×10^{-6}	6.61×10^{-7}	5.97×10^{-6}	1.04×10^{-5}	2.41×10^{-5}	3.78×10^{-4}	1.60×10^{-3}	8.38×10^{-4}	3.92×10^{-4}	1.09×10^{-5}	2.72×10^{-6}	1.43×10^{-6}
	15	1.35×10^{-6}	5.51×10^{-7}	5.86×10^{-6}	9.68×10^{-6}	2.37×10^{-5}	3.75×10^{-4}	1.60×10^{-3}	8.27×10^{-4}	3.84×10^{-4}	1.03×10^{-5}	2.48×10^{-6}	1.21×10^{-6}

Table A5. Summary of the impact of 80% participation rate of optimal PEV charging in 12 months.

Grid Impact	Transformer	January	February	March	April	May	June	July	August	September	October	November	December
Load Surge	1	16.24	16.31	16.14	17.98	22.31	28.13	28.91	28.83	27.6	20.71	15.74	16.44
	4	16.22	16.29	16.13	17.9	22.31	28.16	28.91	28.83	27.6	20.56	15.78	16.18
	6	16.22	16.3	12.96	17.65	22.3	28.19	28.92	28.82	27.61	20.41	15.74	13.49
	8	16.77	17.04	16.34	17.65	22.31	28.19	28.92	28.83	27.61	20.71	22.34	22.78
	12	16.38	16.42	16.19	17.96	21.88	27.52	28.26	28.18	26.94	20.81	16.73	17.5
	15	17.23	16.51	14.55	18.15	22.31	28.13	28.89	28.83	27.59	20.82	16.64	17.5
Minimum line voltage	1	117.5	117.8	117.5	117.6	116.9	115.9	115.7	115.8	116	117.1	117.8	117.7
	4	117.5	117.6	117.5	117.5	116.8	115.8	115.7	115.7	115.9	117.1	117.7	117.7
	6	118.3	118.3	118.4	118.5	117.9	117.2	117.1	117.1	117.3	118.1	118.5	118.6
	8	118.3	118.3	118.3	118.2	117.7	117	116.9	116.9	117.1	117.9	118.1	118
	12	117.3	117.4	117.3	117.4	116.7	115.6	115.5	115.5	115.8	116.9	117.6	117.5
	15	117.3	117.5	117.4	117.4	116.8	115.7	115.6	115.6	115.9	117	117.7	117.5
Transformer Aging—insulation loss of life (%)	1	1.49×10^{-6}	5.88×10^{-7}	3.81×10^{-6}	1.11×10^{-5}	3.03×10^{-5}	5.09×10^{-4}	2.10×10^{-3}	1.10×10^{-3}	4.99×10^{-4}	1.21×10^{-5}	2.66×10^{-6}	1.23×10^{-6}
	4	1.27×10^{-6}	4.93×10^{-7}	3.81×10^{-6}	1.06×10^{-5}	3.01×10^{-5}	5.08×10^{-4}	2.00×10^{-3}	1.10×10^{-3}	4.94×10^{-4}	1.17×10^{-5}	2.49×10^{-6}	1.00×10^{-6}
	6	1.13×10^{-6}	4.84×10^{-7}	4.70×10^{-6}	1.14×10^{-5}	3.45×10^{-5}	5.85×10^{-4}	2.30×10^{-3}	1.20×10^{-3}	5.70×10^{-4}	1.29×10^{-5}	2.56×10^{-6}	8.62×10^{-7}
	8	2.43×10^{-6}	9.97×10^{-7}	8.33×10^{-6}	1.52×10^{-5}	4.05×10^{-5}	4.05×10^{-5}	2.80×10^{-3}	1.50×10^{-3}	6.74×10^{-4}	1.67×10^{-5}	3.81×10^{-6}	2.31×10^{-6}
	12	1.80×10^{-6}	6.71×10^{-7}	5.97×10^{-6}	1.12×10^{-5}	2.82×10^{-5}	6.93×10^{-4}	1.90×10^{-3}	1.00×10^{-3}	4.61×10^{-4}	1.20×10^{-5}	2.88×10^{-6}	1.49×10^{-6}
	15	2.00×10^{-6}	8.17×10^{-7}	5.86×10^{-6}	1.87×10^{-5}	7.17×10^{-5}	1.37×10^{-3}	5.00×10^{-3}	2.80×10^{-3}	1.30×10^{-3}	2.51×10^{-5}	4.06×10^{-6}	1.56×10^{-6}

References

1. United States Environmental Protection Agency (EPA), National Highway Traffic Safety Administration (NHTSA). 2017 and Later Model Year Light-Duty Vehicle Greenhouse Gas Emissions and Corporate Average Fuel Economy Standards. 2011. Available online: https://www.gpo.gov/fdsys/search/pagedetails.action?collectionCode=FR&browsePath=2011%2F12%2F12-01%5C%2F5%2FEnvironmental+Protection+Agency&granuleId=2011-30358&packageId=FR-2011-12-01&fromBrowse=true (accessed on 30 November 2016).
2. U.S. Department of State. United States Climate Action Report (2014 CAR). Available online: http://www.state.gov/e/oes/rls/rpts/car6/index.htm (accessed on 30 November 2016).
3. U.S. Environmental Protection Agency. Inventory of U.S. Greenhouse Gas Emissions and Sinks. 2015. Available online: http://www.epa.gov/climatechange/emissions/usinventoryreport.html (accessed on 30 November 2016).
4. Liu, R.; Dow, L.; Liu, E. A survey of PEV impacts on electric utilities. In Proceedings of the 2011 IEEE PES Innovative Smart Grid Technologies (ISGT), Anaheim, CA, USA, 17–19 January 2011; pp. 1–8.
5. Bosovic, A.; Music, M.; Sadovic, S. Analysis of the impacts of plug-in electric vehicle charging on the part of a real medium voltage distribution network. In Proceedings of the 2014 IEEE PES Innovative Smart Grid Technologies Conference Europe (ISGT-Europe), Istanbul, Turkey, 12–15 October 2014; pp. 1–7.
6. Calderaro, V.; Galdi, V.; Graber, G.; Massa, G.; Piccolo, A. Plug-in EV charging impact on grid based on vehicles usage data. In Proceedings of the 2014 IEEE International Electric Vehicle Conference (IEVC), Florence, Italy, 17–19 December 2014; pp. 1–7.
7. Qian, K.; Zhou, C.; Allan, M.; Yuan, Y. Modeling of Load Demand Due to EV Battery Charging in Distribution Systems. *IEEE Trans. Power Syst.* **2011**, *26*, 802–810. [CrossRef]
8. Rautiainen, A.; Repo, S.; Järventausta, P.; Mutanen, A.; Vuorilehto, K.; Jalkanen, K. Statistical Charging Load Modeling of PHEVs in Electricity Distribution Networks Using National Travel Survey Data. *IEEE Trans. Smart Grid* **2012**, *3*, 1650–1659. [CrossRef]
9. Argade, S.; Aravinthan, V.; Jewell, W. Probabilistic modeling of EV charging and its impact on distribution transformer loss of life. In Proceedings of the 2012 IEEE International Electric Vehicle Conference (IEVC), Greenville, SC, USA, 4–8 March 2012; pp. 1–8.
10. Hilshey, A.D.; Rezaei, P.; Hines, P.D.H.; Frolik, J. Electric vehicle charging: Transformer impacts and smart, decentralized solutions. In Proceedings of the 2012 IEEE Power and Energy Society General Meeting, San Diego, CA, USA, 22–26 July 2012; pp. 1–8.
11. Meyer, D.; Choi, J.; Wang, J. Increasing EV public charging with distributed generation in the electric grid. In Proceedings of the 2015 IEEE Transportation Electrification Conference and Expo (ITEC), Dearborn, MI, USA, 14–17 June 2015; pp. 1–6.
12. Vehicle-Grid Integration: A Vision for Zero-Emission Transportation Interconnected throughout California's Electricity System. 2013. Available online: http://docs.cpuc.ca.gov/PublishedDocs/Published/G000/M080/K775/80775679.pdf (accessed on 30 November 2016).
13. Scholer, R.A.; McGlynn, H. Smart Charging Standards for Plug-In Electric Vehicles. In Proceedings of the SAE 2014 World Congress & Exhibition, Detroit, MI, USA, 8–10 April 2014.
14. Kersting, W.H. *Distribution System Modeling and Analysis*, 2nd ed.; CRC Press: Boca Raton, FL, USA, 2002.
15. American National Standards Institute (ANSI). *American National Standard For Electric Power Systems and Equipment—Voltage Ratings (60 Hertz)*; ANSI C84.1-2011; National Electrical Manufacturers Association: Rosslyn, VA, USA, 2011.
16. GridLAB-D. Available online: http://www.gridlabd.org/ (accessed on 30 November 2016).
17. Florida Public Service Commission. Report on Electric Vehicle Charging. Tallahassee, FL, USA. 2012. Available online: http://www.freshfromflorida.com/content/download/11426/144852/Electric_Vehicle_Charging_Report.pdf (accessed on 30 November 2016).
18. National Highway Traffic Safety Administration (NHTSA). National Household Travel Survey. Available online: http://nhts.ornl.gov/index.shtml (accessed on 30 November 2016).
19. CEl-Bayeh, L.Z.; Mougharbel, I.; Saad, M.; Chandra, A.; Lefebvre, S.; Asber, D. A detailed review on the parameters to be considered for an accurate estimation on the Plug-in Electric Vehicle's final State of Charge. In Proceedings of the 2016 3rd International Conference on Renewable Energies for Developing Countries (REDEC), Beirut, Lebanon, 13–15 July 2016; pp. 1–6.

20. SAE World Congress. J1772-SAE Electric Vehicle and Plug in Hybrid Electric Vehicle Conductive Charge Coupler. 2010. Available online: http://standards.sae.org/wip/j1772/ (accessed on 30 November 2016).
21. IEEE Power & Energy Socierty (PES). IEEE 13 Node Test Feeder. Available online: http://ewh.ieee.org/soc/pes/dsacom/testfeeders/index.html (accessed on 30 November 2016).
22. Kersting, W.H. Radial distribution test feeders. In Proceedings of the IEEE Power Engineering Society Winter Meeting, Columbus, OH, USA, 28 January–1 February 2001.
23. Office of Energy Efficiency & Renewable Energy (EERE). Commercial and Residential Hourly Load Profiles for all TMY3 Locations in the United States. Available online: http://en.openei.org/doe-opendata/dataset/commercial-and-residential-hourly-load-profiles-for-all-tmy3-locations-in-the-united-states (accessed on 30 November 2016).
24. C57.91-2011—IEEE Guide for Loading Mineral-Oil-Immersed Transformers and Step-Voltage Regulators. 2012. Available online: http://ieeexplore.ieee.org/servlet/opac?punumber=6166925 (accessed on 30 November 2016).
25. Gönen, T. *Electric Power Distribution System Engineering*, 3rd ed.; CRC Press: Boca Raton, FL, USA, 2008.
26. GridLAB-D: Power Flow User Guide. Available online: http://gridlabd.me.uvic.ca/wiki/index.php/Power_Flow_User_Guide (accessed on 30 November 2016).

© 2016 by the authors; licensee MDPI, Basel, Switzerland. This article is an open access article distributed under the terms and conditions of the Creative Commons Attribution (CC-BY) license (http://creativecommons.org/licenses/by/4.0/).